Engineering the Size of DNA Repair Inhibitor-Encapsulated Polymeric Nanoparticles to Improve the Therapeutic Index of Chemoradiotherapy

Stephanie Yu

Senior Honors Thesis
Gillings School of Global Public Health
Department of Environmental Sciences and Engineering
University of North Carolina at Chapel Hill

In Collaboration with
Lineberger Comprehensive Cancer Center
University of North Carolina Healthcare
Department of Radiation Oncology

Spring 2017

Approved by:

_____

Advisor: Andrew Wang
Reader: Avram Gold
Reader: Rodger Sit

Dedication

To Ian Maynor, Katrina Gutierrez, Jonathan Chan, Arnab Chatterjee, and Xiaoyan Han. When I told you my wildest and most improbable dreams, you told me to forget it and go work at the high paying tech company instead. I ignored you, but it motivated me to work even harder to get to where I want to go. I will hold onto that strength until I get to rub it in your faces. With love, of course.

But in all seriousness, the 2 am movies, 3 am pizza, 4 am freak out phone calls, along with everything else we shared is what got me through all the rough times and made the good times even better. I love you all so much and can never thank you enough for your love and support.

To my sister, Christina Yu, and my cousins, Jennifer Yu and Samantha Yu, I love you all so much, and the thoughts of you drive me to succeed as both a scientist and as a role model. Here's to hoping you all pursue careers in STEM.

To my dear, departed cousin, Anna Ha. You were the first person in the family I could be completely open and honest with. I wouldn't be who I am today without you. I love you so much and am so grateful for our time together, short though it was. Rest in peace.

Acknowledgements

My advisor:

Dr. Andrew Wang – I can never thank you enough for your impeccable mentorship, leadership, and support. When I first joined your lab, I told you I would never go into medicine. You said you would change that, and I secretly laughed. Today, I am on a mission to become half the physician, scientist, mentor, and friend that you are. Also, for your (slightly intimidating) critiques of us during lab meeting that forged me into a better scientist.

My committee members:

Dr. Avram Gold and Dr. Roger Sit – for taking time out of your busy schedules to be a part of my thesis and defense, and for your support, encouragement, and suggestions throughout the process.

Past and present members of the Wang lab:

Special thanks to Dr. Joseph Caster, Dr. Xi Tian, Dr. Yanfei Qi, Dr. Kyle Roche, and Kyle Wagner for your guidance, mentorship, and patience. Sam Warner, Nikki Newman, Artish Patel, and Zach Lee – thank you for making the more tedious parts of experiments and data collection more bearable with our discussion, debates, and jokes both in and out of lab.

My friends, classmates, and teachers:

Mitch Xia –for your encouragement and constant nudges while I procrastinated during the last few days before my deadline. Lily Huang, Rosa Yang, Jun Huo, and Linda Vue – you were there when I started thinking about STEM as a career and was struggling to understand basic science, but you never judged me or let me give up. Evan Teng, Snigdha Das, Nick Hatcher, Vimy Dang, Keith Kariuki, and Adam Aji – for believing in me and continuing to support me when I didn't believe in myself and for countless memories of food at absurd hours. Samuel Lee, Su Cho, Tammy Yu, and Derek Chan – for being there from the beginning until now and reminding me of where I came from and how I've grown. Jonathan Rader and Pranav Khandelwal – for geeking out with me about cool new science discoveries and high impact factor papers that will one day be ours. Jack Whaley, Dr. Brian Hogan, Dr. Frank Church, Dr. Diane Pozefsky, Dr. John Morrison, Dr. Gary Bishop, Jon Davis, and Therese Taxis – for going above and beyond what most teachers and professors do, and taking extra time to ensure I was making responsible decisions and to guide me throughout my academic career.

Table of Contents

Abstract

Nanoparticle (NP) delivery of chemotherapeutic drugs can be used to both improve tumor toxicity and reduce toxicity to normal tissue in chemo and chemoradiotherapy (CRT). However, various properties of nanoparticles with respect to CRT are yet to be explored. For instance, it is unknown how particle size may affect the therapeutic index of CRT. Exploration of this topic may provide invaluable insight on how NP-based CRT could be administered clinically in the future, as there is currently no set standard on an optimal particle size. PEG-PLGA nanoparticles were engineered encapsulating either the DNA-PK inhibitor Wortmannin (wtmn) or the ATM inhibitor KU60019 of various sizes (50, 100, or 150 nm in diameter) and studied their biodistribution, efficacy, and toxicity in CRT. Effects *in vitro* were observed in three colorectal adenocarcinoma lines (HT-29, SW480, and LoVo) and *in vivo* in mice. These nanoformulations were shown to be both cytotoxic and radiosensitizing in these cell lines, and there was no effect of particle size on toxicity *in vitro*. The largest particles were most rapidly cleared by the liver, but still penetrated tumors well *in vivo*. All sizes of nanoformulations were effective radiosensitizers of rectal tumor xenografts *in vivo*. In no instance did the largest or smallest particles appear to demonstrate any greater efficacy than medium sized particles when combined with radiation. The 50 nm KU60019 particles caused greater bowel toxicity than larger particles, and the 100 nm Wortmannin particles induced significantly more radiosensitization than larger or smaller particles in SW480 xenografts, a trend that was also observed in most other tumor/drug combinations. Radiation-induced rectal toxicity was minimal in animals treated with all three particle sizes. There was also no significant effect of particle size on hematologic of hepatotoxicity. These results demonstrate that particles in the 100 nm size range may be optimal for clinical applications in chemoradiotherapy.

Introduction

Background

Historically, several drugs with the potential to be used as powerful chemotherapeutics were abandoned in clinical development due to high toxicity to normal tissue or poor stability or solubility in blood. For instance, Wortmannin, despite being a potent anti-cancer agent, was deemed too hepatotoxic for patient use and demonstrated poor solubility and stability in preclinical studies. Because traditional chemotherapies are system-wide, they are not targeted towards a primary tumor; thus, toxicity to normal tissue is strictly monitored.[1] This problem remains an issue for drugs approved for chemotherapy, as patients may have adverse reactions to the drugs and must stop treatment before they can effectively treat their cancer. As such, the search to find a targeted way to treat cancers while minimizing damage to normal tissue is crucial.

Targeted chemotherapy in the form of polymeric nanoparticle drug delivery is a method currently being studied for its ability to increase effectiveness against cancerous tumors while minimizing normal tissue toxicity. Several types of cancers, including many rectal cancers, have defective vasculature serving the primary tumor. This leaky vasculature combined with poor lymphatic draining systems, allows for less selective permeability and greater retention of materials into the tumor.[2] Nanoparticles are then able to better penetrate cancerous tumor vasculature than that of normal tissue. Nanoparticle formulation of drugs like Wortmannin showed decreased toxicity, increased stability and solubility, and increased effectiveness as an anti-cancer agent in preclinical studies.[1]

Chemoradiotherapy

CRT is used to treat various types of solid cancers, including those of the rectum, lungs, esophagus, and head and neck.[3] Radiosensitizers, which improve the efficacy of radiotherapy, are

often given concurrently with radiation.[4] While this improves efficacy, it often comes at the price of excess toxicity as normal tissues are also sensitized to radiation. Several pre-clinical studies have demonstrated that nanoformulations of radiosensitizers can improve the therapeutic index of chemoradiotherapy by improving tumor-specific delivery of the drug and reducing normal tissue exposure.[1] These studies suggest that the rational development and translation of radiosensitizing nanoformulations can improve clinical outcomes for cancer patients.

One critical limitation to the development and translation of nanotherapeutics for use as radiosensitizers is that very little is currently known about the optimal particle characteristics for this indication. Physical characteristics, such as particle size, can drastically affect biodistribution and other important pharmacokinetic properties. It is generally believed that nanoparticles in the sub-50 nm range are desirable as drug delivery vehicles since they should rapidly penetrate tumors and be cleared less quickly than larger particles.[5] However, it is unclear if these properties are desirable in chemoradiotherapy applications in which the goal is to maximize differences between normal tissue and tumor drug concentrations. Since radiation is the predominant source of local tumor damage in chemoradiotherapy, it is possible that larger particles (100 – 150 nm) may be equally if not more efficacious with less toxicity to normal tissue than smaller particles. By examining the relationship between particle size and therapeutic index, a rational design for nanoparticle drug formulations may be optimized for use in chemoradiotherapy.

In this study, the efficacy and toxicity of polymeric (mPEG-PLGA) nanoformulations of the DNA repair inhibitors Wortmannin and KU60019 of three different sizes (50, 100, and 150 nm) were compared in mouse models of colorectal cancer. Wortmannin is a potent inhibitor of DNA-PK and PI3 kinase.[6] KU60019 specifically inhibits ATM, a protein kinase recruited and activated by double-stranded breaks in DNA.[7] The efficacy, toxicity, and biodistribution of these

three distinct nanoformulations were compared when combined with radiation in mouse xenograft models of colorectal cancer.

Materials and Methods

Materials

KU60019 and Wortmannin were purchased from Apex Bio (Houston, Texas). Methoxy-poly(ethylene glycol)-block-poly(lactic-co-glycolic acid) (mPEG-PLGA) with molecular weights of 2000:15,000 Da (PEG(2K):PLGA(15K)) and 5000:10,000 Da (PEG(5K):PLGA(10K)) were purchased from PolySciTech (West Lafayette, IN). Poly(D,L-lactic acid) (PLA) with an average molecular weight of 18,000 – 28,000 was purchased from Sigma-Aldrich (St. Louis, MO). Acetonitrile (HPLC grade) and double distilled water (HPLC grade) were purchased from Sigma-Aldrich (St. Louis, MO). Flamma Fluor (FKR648) was purchased from Akina, Inc. (West Lafayette, IN).

Nanoparticle Preparation

Nanoprecipitation was used to create nanoparticles of each of the different sizes. Polymers and drugs were dissolved in ACN (mPEG_PLGA at 40 mg/mL; PLA, KU60019, Wortmannin at 2 mg/mL). Drug-polymer mixtures brought to a final volume of 1 mL in ACN were added dropwise to 3 mL double deionized water over rapid stirring (800 – 1200 rpm) at room temperature. The mixture was constantly stirred under vacuum at room temperature for 3 hours to allow self-assembly and evaporation of the organic solvent (ACN). Nanoparticles were then centrifuged for 15 min at 8000 x G in 30 KDa cut-off centrifuge filters (Millipore, Billerica, MA), washed in 1 mL 1x Dulbecco's phosphate-buffered saline (DPBS) followed by repeat centrifugation. After three washes, the particles were resuspended to desired concentrations in 1x DPBS or tissue culture media.

Nanoparticle size was adjusted by modifying polymer compositions within the ACN. 50 nm particles were obtained by adding 5 mg of 5000:10,000 mPEG-PLGA and 500 µg (10%) drug. 100 nm particles were generated by adding 5 mg 2000:15,000 mPEG-PLGA, 3 mg PLA, and 800 µg (10%) drug. 150 nm particles were created by adding 7 mg 2000:15,000 mPEG-PLGA, 9 mg PLA, and 800 µg (5%) drug. Drug-free particles of each size were created by bringing polymeric solutions to volume.

Nanoparticle Characterization

Purified nanoparticles encapsulating Wortmannin or KU60019 were characterized by transmission electron microscopy (TEM), dynamic light scattering, and aqueous electrophoresis. Prior to TEM imaging, concentrated NP samples were diluted to 5 mg/mL in deionized water. A 5 µL sample of each was mixed with 5 µL 4% uranyl acetate aqueous solution before being added to a 400 mesh carbon-filmed copper grid. TEM images were captured using a Zeiss TEM 910 transmission electron microscope operated at 80 kV (Carl Zeiss Micrscopy, LLC, Thornwood, NY) in the Microscopy Services Laboratory core facility at the UNC School of Medicine. Intensity-average diameter and mean zeta potential (ζ) of nanodispersions were determined by dynamic light scattering and an aqueous electrophoresis method using a Zetasizer Nano ZS instrument (Malvern Inc, Worcestershire, UK). All measurements were based on the average of three separate measurements.

Drug Loading Efficiency

Loading efficiency of KU60019 or Wtmn in the nanoparticles was measured with a Shimadzu SPD-M20A high pressure liquid chromatography (HPLC) system (Shimadzu, Kyoto, Japan) equipped with a diode array detector at a GP-C18 reverse phase column (pore size = 120 A, 4.6 x 150 nm, Sepax Technology, Newark DE). For preparation, 100 µL of purified particles

was dissolved in 100 µL of ACN, vortexed vigorously, and stored over night at 4°C to allow complete dissolution of particles. Drug concentrations were determined by generating standard curves from 0 – 100 µM for each drug. A linear gradient from 10% ACN in water to 100% ACN was run over 15 min, followed by 100% ACN for 5 min, then 10% ACN for 5 min. Flow rate used was 1 mL/min. Wtmn eluted with a retention time of 5.6 min and was detected at a wavelength of 250 nm. KU60019 eluted with a retention time of 6.4 min and was detected at a wavelength of 230 nm. Drug loading (wt/wt%) was calculated as (wt drug mg/wt polymer mg) x 100%. Encapsulation efficiency was calculated as (concentration of drug in dissolved particles/concentration of drug in initial organic phase solution) x 100%.

Drug Release Studies

Release rates of the drugs were measured using 100 µL of purified nanoparticles diluted to 2.5 mg/mL into Slide-A-Lyzer MINI dialysis tubes with a molecular weight cut-off of 10 kDa (Pierce, Rockford, IL) and dialized against 4 L of 1x DPBS with gentle stirring (50 rpm) at 37°C. At selected times (0, 1, 3, 6, 12, and 24 hours for Wtmn, 0, 1, 2, 3, 6, 12, 24, 48, and 72 hours for KU60019), the entire sample in a dialysis tube was removed and dissolved in equal parts ACN to allow dissolution overnight. Drug concentrations were determined using HPLC, as described above. Drug loading and encapsulation efficiency were determined at time 0 (immediately after initial purification). Drug release half-time ($T_{1/2}$) is defined as the time for half the encapsulated drug to be released and was calculated using GraphPad Prism software V4.0 (La Jolla, CA).

In Vitro Studies

Cell Culture: Human colorectal adenocarcinoma cell lines HT-29, SW480, and LoVo were collected from the University of North Carolina tissue culture facility in the Lineberger Comprehensive Cancer Center. Cells were cultured using Dulbecco's Modified Eagle Medium

(DMEM): Nutrient Mixture F-12 (Gibco, Thermo Fisher Scientific, Waitham, MA) supplemented with 10% (v/v) Fetal Bovine Serum (FBS) and 1% penicillin/streptomycin.

MTS Cell Viability Assays: *In vitro* toxicities of the different sized nanoparticles of KU60019 and Wtmn were determined using MTS cell viability assays. Cells were plated in 96 well plates at densities of 10,000 cells per well, left to adhere overnight, then treated with varying concentrations of drugs. For cells treated with Wtmn, drug was removed after 3 hours, and cells were washed twice with sterile DPBS and grown in fresh media for 48 hours at 37°C. For cells treated with KU60019, drug was removed after 24 hours, and cells were washed twice with sterile DPBS, and grown in fresh media for another 24 hours at 37°C. Cell viability was assessed using MTS reagent (Promega, Madison WI). Absorbance was recorded at 492 nm using a 96-well plate reading (Infinite 200 Pro, Tecan i-control). Relative cell survival was determined by dividing the intensity of each well by the average intensity obtained in wells containing cells treated without drug multiplied by 100. All conditions were done in triplicate.

Clonogenic Cell Survival Assays: *In vitro* radiosensitization effects of KU60019 and Wtmn were determined using clonogenic cell survival assays. Cells were cultured at densities ranging from 100 – 40,000 cells per dish for 24 hours. Media was then replaced with media containing varying concentrations of NP-encapsulated drugs. Cells treated with KU60019 (2.5 μM for HT-29 and SW480, 1.5 μM for LoVo) were radiated with 0, 2, 4, 6, or 8 Gy of radiation after 3 hours, then left with media unchanged for an additional 21 hours for a total of 24 hours. Media was then removed, and cells were washed twice with sterile DPBS and cultured in fresh media at 37°C for 12 days. For Wtmn experiments, cells were treated with media containing free or NP Wtmn (equivalent to 20 μM for HT-29 and SW480, 15 μM for LoVo) for 3 hours followed by the same doses of radiation. Cells were then washed twice with sterile PBS and cultured in fresh media at

37°C for 12 days. Cells were then fixed in a 4% (v/v) neutral buffered formalin solution and stained with trypan blue. All colonies with at least a single cell were counted. All conditions were done in triplicate.

In Vivo Studies

Mice were maintained in the Center for Experimental Animal Studies (an AAA LAC-accredited experimental animal facility) at the University of North Carolina. All procedures involving mice were done in accordance with protocols approved by the University of North Carolina Institutional Animal Care and Use Committee (IACUC) and conformed to the Guide for the Care and Use of Laboratory Animals (NIH publication no. 86 – 23). Athymic nude mice were obtained from UNC animal services core (Chapel Hill, NC). C57bl/6J mice were obtained from Jackson Labs (Barr Harbor, ME).

Antitumor Efficacy: Xenograft tumors were injected into the left flanks of male nude athymic mice (6 – 7 weeks old, 28 – 30 g). For HT-29, mice were inoculated with 1 x 10^6 cells in a 1:1 mixture of plain DMEM F-12 media:matrigel mixture. The average tumor volume after 7 days was 200.0 mm^3. For SW 480, mice were inoculated with 2.25 x 10^6 cells in a 1:1 mixture of plain DMEM F-12 media:matrigel mixture. Average tumor volume after 10 days was 166.3 mm^3. For these experiments, a fractionated radiation schedule with repeated dosing of NPs was utilized. This type of treatment schedule is clinically relevant as radiation is most frequently given in a fractionated manner. Further, radiation is known to affect vascular permeability and structure[8] which could in turn affect anti-tumor efficacy or toxicity of particles in a size-dependent manner.

On the first day of treatment (7 days after inoculation for HT-29, 10 days after inoculation for SW480), animals were injected with saline or NP drug (50, 100, 150 nm formulations) via tail vein injection (0.07 mg/kg Wtmn and 0.5 mg/kg KU60019). Three hours after injection, tumors

were irradiated at 5 Gy using a Precision X-Ray: X-RAD 320 irradiation system (Precision X-Ray Inc) operating at 320 KVp and 12.5 mA. The source-surface distance was 47 cm at a dose rate of 100 cGy/min. For radiation, the tumors were left exposed and mice were shielded with 4 mm of lead. On the second day, animals were again treated with 5 Gy of radiation with no drug. On day 3, animals were again injected with saline or NP drug and treated with 5 Gy radiation 3 hours later. To test the effects of particle size on chemotoxicity without radiation, a separate control group of mice were treated with saline or NP formulations on days 1 and 3 with no radiation. Tumor volume was measured every 3 days via manual caliper measurements in two perpendicular directions. Tumor volume was calculated as $0.5 * x * y^2$, where x is the larger dimension and y is the smaller dimension. Mice were euthanized by CO_2 overdose when tumors exceeded 20 mm in greatest dimension or reached 3500 mm^3 in volume.

Toxicity: Histologic assessment of small bowel crypt density following CRT was used to quantify gastrointestinal (GI) toxicity. Small bowel was selected as it is frequently the dose-limiting structure in pelvic/abdominal CRT.[9] Tumor-free C57bl/J6 mice were treated with saline or NP injections on days 1 and 3 (using the same treatment schedule as that of the *in vivo* tumor efficacy studies) and 3 daily doses of 5 Gy whole abdominal radiation. Mice were euthanized 48 hours after the final radiation fraction, and distal ilium were harvested and fixed in 4% neutral buffered formalin solution overnight, then stored in 70% ethanol prior to being embedded in paraffin and processed at the University of North Carolina tissue core facility. Immunostainings of paraffin-embedded samples were performed, and antigen retrieval was accomplished by boiling samples in a 10 mM sodium citrate buffer at pH 6.0 for 20 min. Samples were incubated with rabbit anti-mouse EpCam antibody (1:100, Abcam). Stainings were visualized with Alexa 488-

conjugated secondary goat antibodies (molecular probes) and nuclei were counterstained with DAPI (molecular probes).

Effects of nanoparticle size on systemic toxicities of Wtmn and KU60019 were measured by analyzing complete blood count (CBC with differential) and hepatotoxicity in tumor-free 8 – week old C57bl/6J mice treated with the various sized particle formulations on days 1 and 3 without radiation. Mice were anesthetized with a ketamine/xylazine solution 48 hours after the final inection and blood was collected through cardiac puncture. A 100 µL sample of whole blood was stored in EDTA-coated tubes at 5°C prior to analysis at the University of North Carolina Animal Clinical Core Facility. For hepatotoxicity, a 400 µL sample of whole blood was transferred to a serum separator tube and stored at room temperature for 30 min followed by centrifugation at 5000 x G for 10 min to separate plasma from the cellular components. Isolated plasma was stored at 5°C prior to analysis at the UNC Animal Clinical Core Facility. Pink samples (indicating hemolysis) and sample readings which exceeded 3 standard deviations of the mean were presumed to be hemolyzed and discarded, as hemolysis can contaminate samples with target enzymes coming from somewhere besides the liver (n = 2 for saline treated mice and n = 1 for all other groups).

Biodistribution: Nude mice were inoculated with HT-29 xenografts (1 x 10^6 cells). Seven days after inoculation, the average tumor size was 150 mm^3. Tumors were treated with 3 daily doses of 5 Gy radiation. After the third fraction of radiation, the mice were injected with saline or 165 mg/kg Flamma Fluor-labeled nanoparticles by IV tail vein injection. Anesthetic overdose was administered, and the animals were decapitated to harvest target organs (heart, liver, spleen, tumor xenograft) 1, 3, 6, 12, and 24 h after injection for *ex vivo* imaging. Fluorescent images were obtained using an IVIS Living Image system (Caliper Life Science, Hopkiton, MA) equipped with

an excitation filter of 640 nm and an emission filter of 680 nm in the University of North Carolina Small Animal Imaging Facility. Region of interest values were recorded as photon flux in total photon count per cm^2 per steradian.

Statistical Analysis

In vitro cytotoxicity was assessed using two-way analysis of variance (ANOVA) using Prism software (Carlesbad, CA) with particle size and drug concentration as variables. Clonogenic cell survival assays were plotted in a linear quadratic regression calculated using CS Cal clonogenic survival calculation software pack. Hematologic and hepatotoxicity were assessed using one-way ANOVA of particle size Post-hoc analysis were performed with Tukey's *t* test when significant main effects were identified. *In vivo* tumor growth was assessed using area under the curve analysis with R software.

Results

Nanoparticle Size Distribution

Nanoparticle KU60019 and Wtmn were engineered with average sizes of 50, 100, and 150 nm by altering polymeric compositions. The nanoprecipitation method produced monodisperse populations of nanoparticles with polydispersity indices (PDIs) of less than 0.1. Table 1 shows the polymeric formulations used to generate each size as well as the mean particles sizes and PDIs. Figure 2 shows representative TEM images of Wtmn and KU60019 nanoformulations, size distribution plots showing virtually no overlap between the largest and smallest sized particles, and release rates for all three sizes of both drugs demonstrating almost identical release rates.

Formulation	Mean Diameter	PDI
5000:10000 Da PEG-PLGA 10% Wtmn	48.4 +/- 1.1 nm	0.07 +/- 0.02
2000:15000 Da PEG-PLGA 38% PLA 10% Wtmn	101.5 +/- 2.1 nm	0.06 +/- 0.02

2000:15000 Da PEG-PLGA 56% PLA 5% Wtmn	147.3 +/- 2.4 nm	0.08 +/- 0.04
5000:10000 Da PEG-PLGA 10% KU600019	44.3 +/- 0.9 nm	0.07 +/- 0.03
2000:15000 Da PEG-PLGA 38% PLA 10% KU60019	94.6 +/- 1.8 nm	0.08 +/- 0.02
2000:15000 Da PEG-PLGA 56% PLA 5% KU60019	138 +/- 2.4 nm	0.09 +/- 0.03

Table 1. Polymeric nanoparticle composition and physical characteristics.

In Vitro Efficacy

Nanoformulations of Wtmn and KU60019 showed comparable levels of cytotoxicity in the absence of radiation (figure 2, top panels). The IC90 for both drugs was about 20 μM in HT-29 and SW480 cells and about 10 μM in LoVo. Particle size did not affect cytotoxicity *in vitro*.

Wtmn particles potential sensitized all three cell lines to radiation at doses corresponding to roughly the IC90. Cells treated with KU60019 particles showed significantly more potent radiosensitization in comparision to Wtmn *in vitro,* and drug dose was reduced to nearly $1/10^{th}$ the IC90 in order to observe enough colony formation to permit quantification. Again, there was no significant effect of particle size for either drug (figure 2, bottom panels).

In Vivo Efficacy

Antitumor efficacy of particles as both chemotherapeutics and as radiosensitizers were tested by injecting mice with HT-29 or SW480 xenografts and treatments of equivalent doses of each of the different sized NPs. All nanoformulations had little to no effect on tumor growth in the absence of radiation (figure 3). By comparison, nanoformulations of both drugs demonstrated potent radiosensitization to both types of tumors (figure 4). There was a slight trend ($P < 0.10$) of improved sensitization with 100 nm nanoparticles in both xenograft models with both drugs. Treatment with the 50 nm particles did not result in greater antitumor efficacy than the larger particles *in vivo* in any cases.

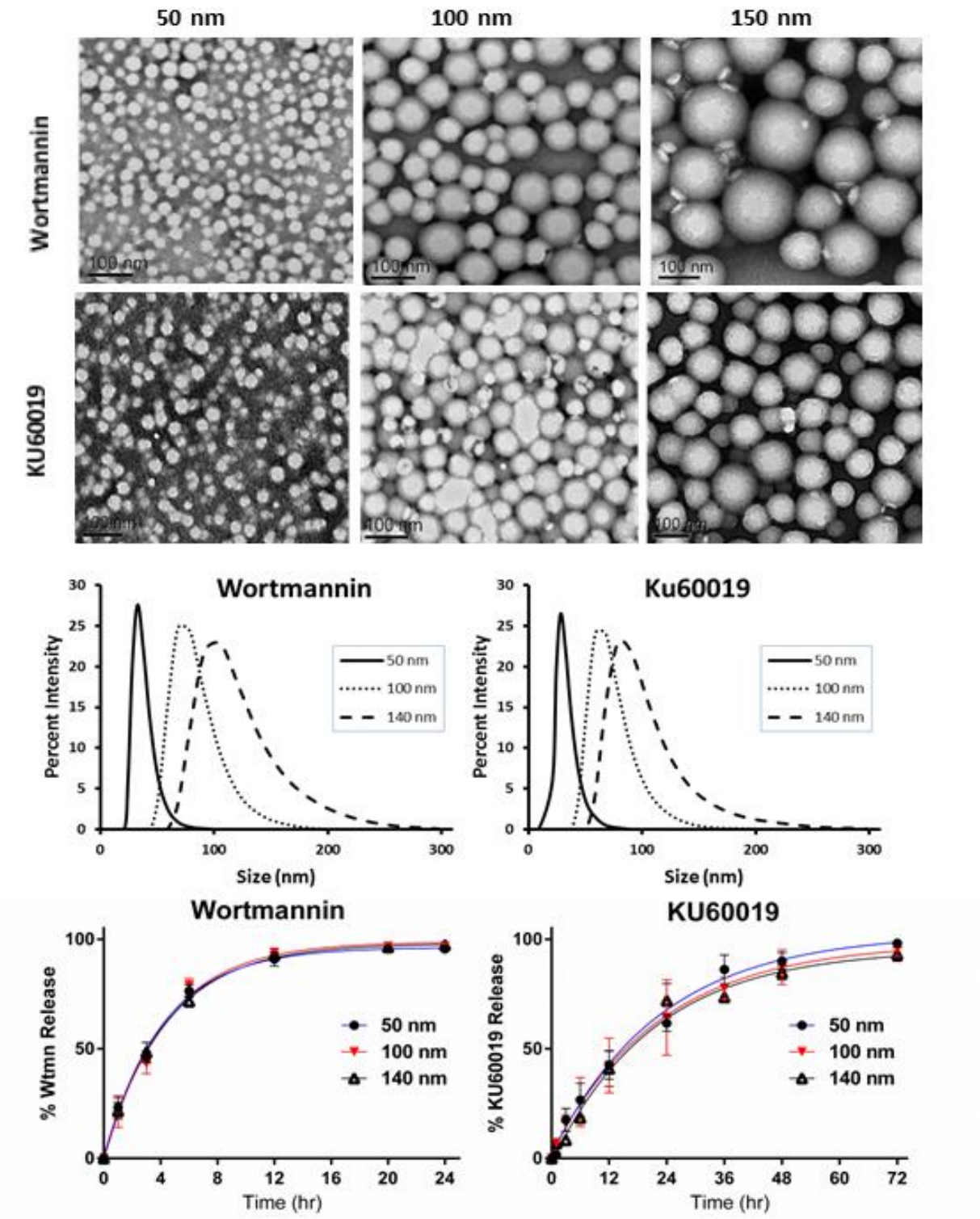

Figure 1. Top: TEM images of Wortmannin and KU60019 nanoparticles. Middle: Size distribution plots demonstrating virtually no overlap between the largest and smallest sized particles. Bottom: All three sizes had similar release rates for both drugs.

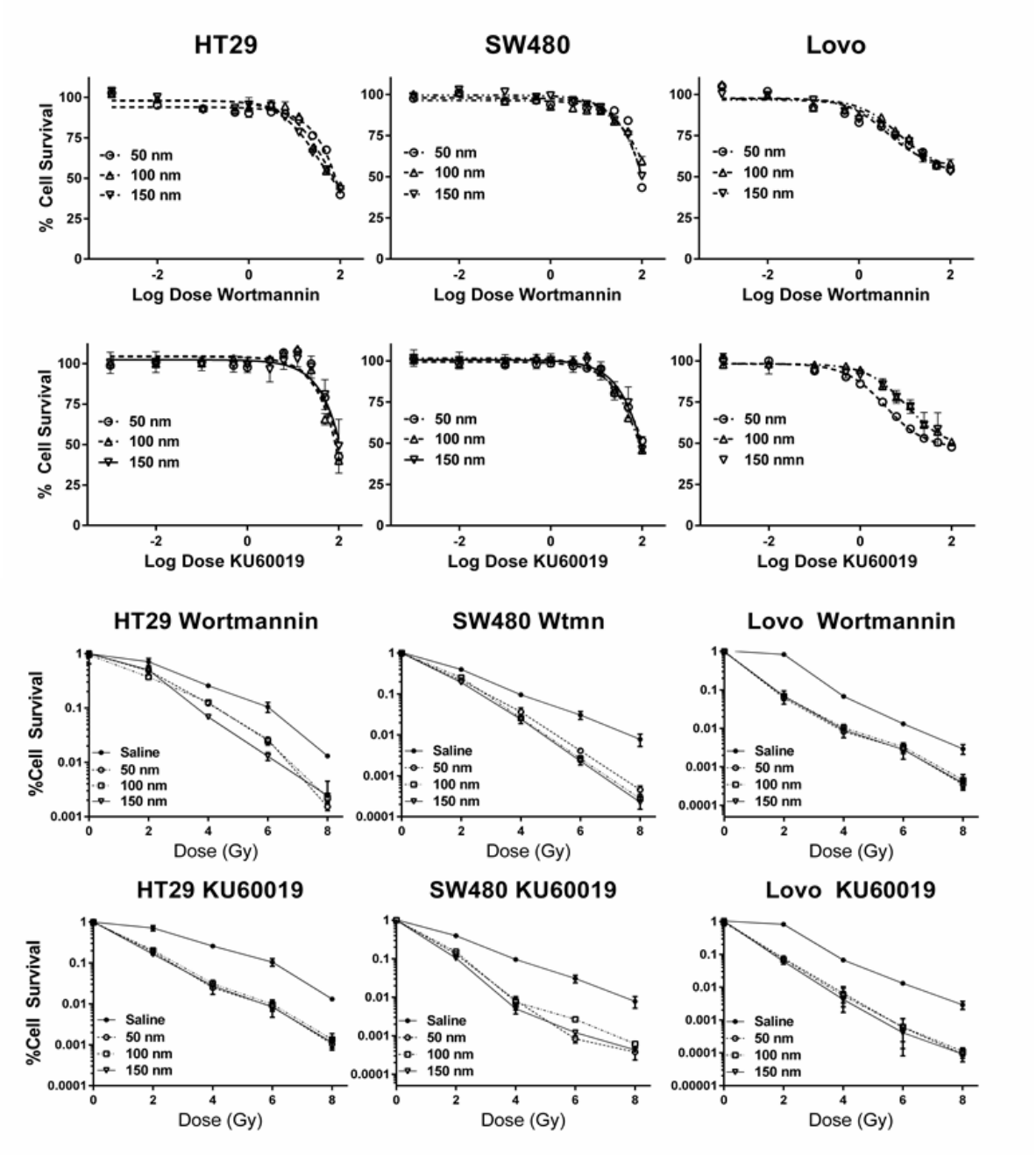

Figure 2. *In vitro* efficacy of drug-loaded NPs. Top two panels: Toxicity of drug-loaded particles without radiation in three rectal cancer cell lines. Bottom two panels: Radiosensitization of rectal cancer cell lines by polymeric Wtmn and KU60019 nanoparticles.

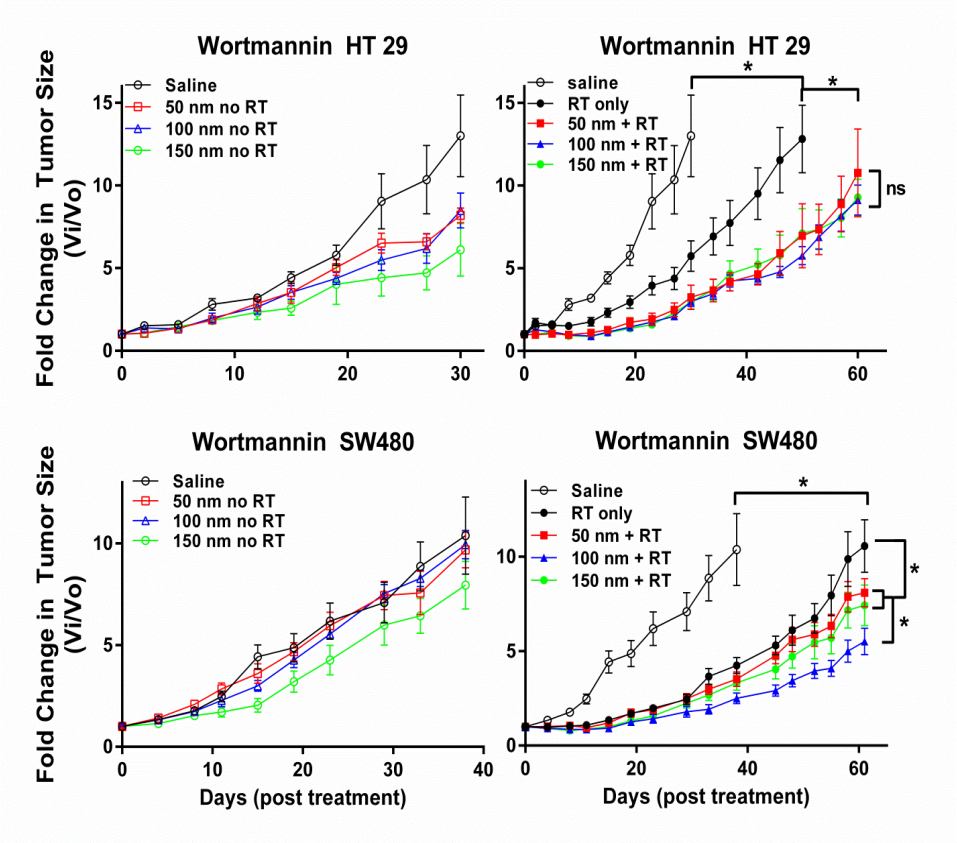
Wortmannin HT 29
Saline
50 nm no RT
100 nm no RT
150 nm no RT
Fold Change in Tumor Size (Vi/Vo)
Wortmannin HT 29
saline
RT only
50 nm + RT
100 nm + RT
150 nm + RT
*
*
ns
Wortmannin SW480
Saline
50 nm no RT
100 nm no RT
150 nm no RT
Fold Change in Tumor Size (Vi/Vo)
Days (post treatment)
Wortmannin SW480
Saline
RT only
50 nm + RT
100 nm + RT
150 nm + RT
*
*
*
Days (post treatment)

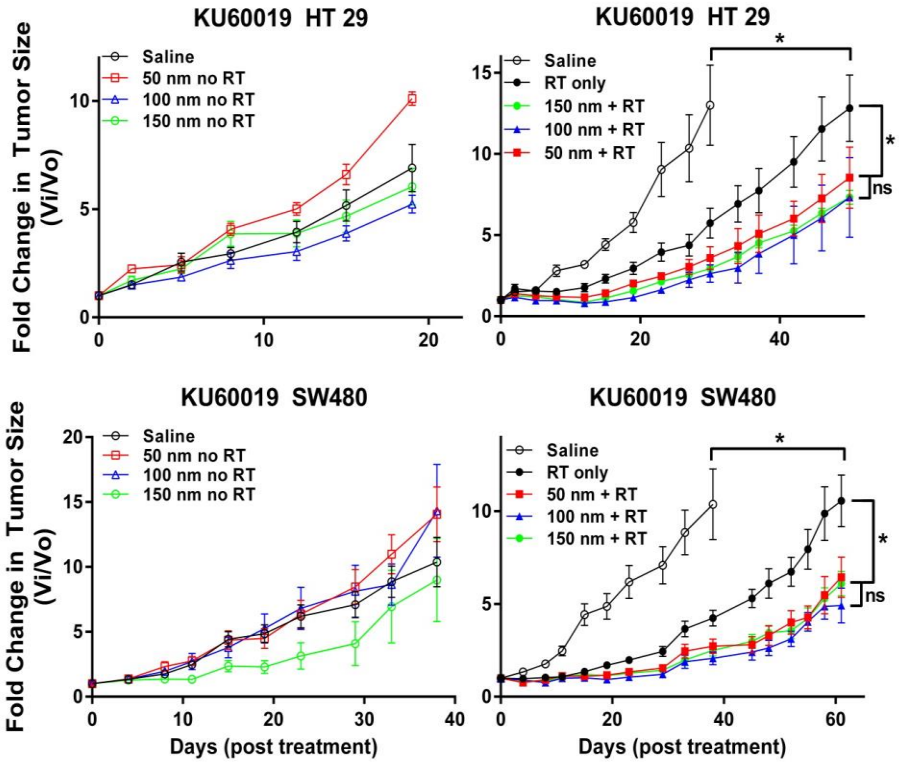
KU60019 HT 29
Saline
50 nm no RT
100 nm no RT
150 nm no RT
Fold Change in Tumor Size (Vi/Vo)
KU60019 HT 29
Saline
RT only
150 nm + RT
100 nm + RT
50 nm + RT
*
*
ns
KU60019 SW480
Saline
50 nm no RT
100 nm no RT
150 nm no RT
Fold Change in Tumor Size (Vi/Vo)
Days (post treatment)
KU60019 SW480
Saline
RT only
50 nm + RT
100 nm + RT
150 nm + RT
*
*
ns
Days (post treatment)

Figure 3. *In vivo* efficacy of drug-loaded nanoparticles without radiation. Tumor growth curves of mice bearing HT-29 (left panels) or SW480 (right panels) xenografts treated with Wtmn (top panels) or KU60019 (bottom panels) nanoparticles. Black circles represent saline treated controls. Red open circles represent mice treated with 50 nm NPs. Blue triangles represent mice treated with 100 nm NPs. Purple triangles represent animals treated with 150 nm NPs.

In Vivo Toxicity

Small bowel crypt density was measured to quantify GI toxicity 48 h after the final fraction of whole abdominal radiation (figure 4). Radiation with free drugs produced a substantial decrease in crypt density, while nanoformulation largely reduced the synergistic toxicity between drug and radiation. There was no significant effect of particle size in the Wtmn nanoparticles, while only the 50 nm KU60019 were more toxic than the larger particles.

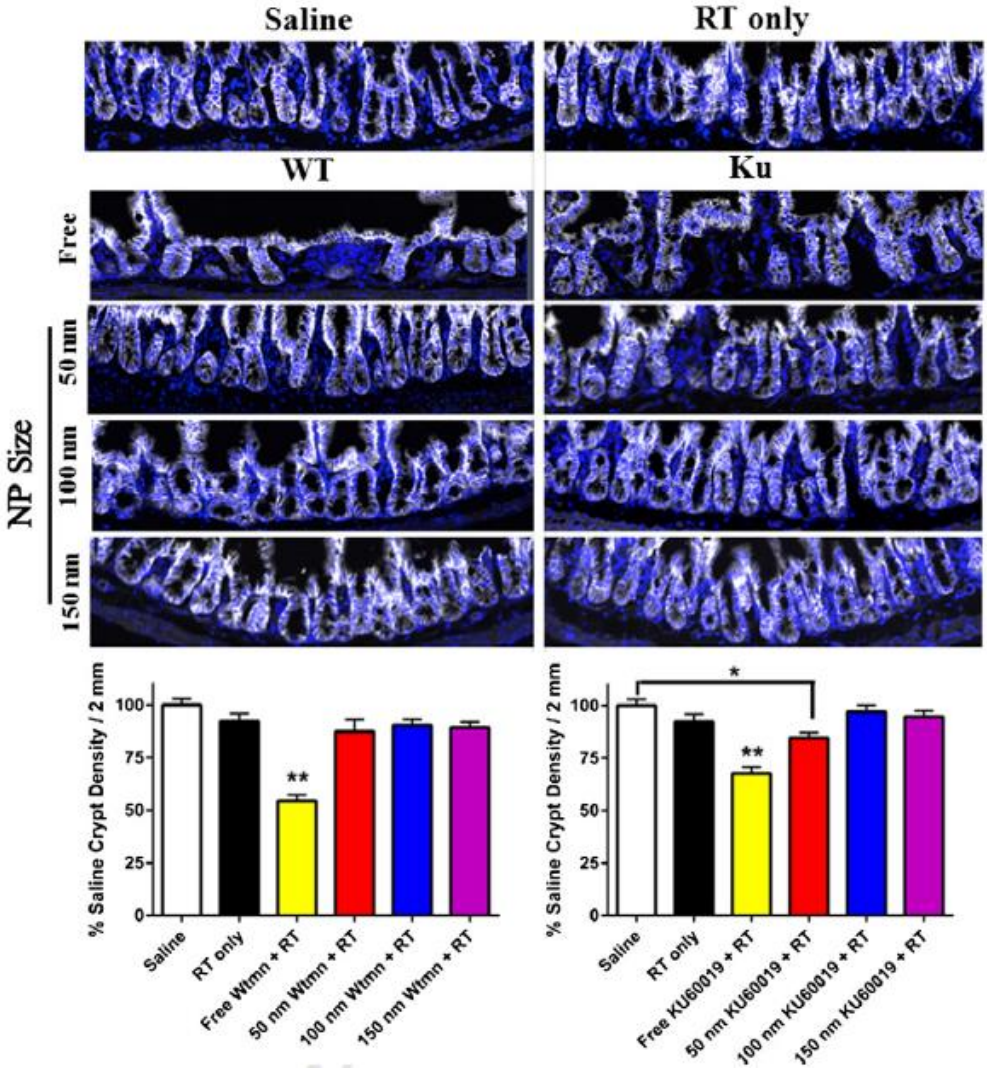

Figure 5. Radiosensitization demonstrating effect of nanoparticle size *in vivo*. *Significantly different from indicated groups. NS non-significant.

Hematologic and hepatic toxicities of each drug were assessed 48 h after treatment with two injections of nanoparticles (days 1 and 3) without radiation (table 2). Hepatotoxicity is a major barrier to the use of Wtmn clinically as a chemotherapeutic.[1] NP formulation greatly reduced this effect, with greater AST and ALT levels in mice with NP Wtmn in comparison to saline, but not significantly ($P < 0.23$). Treatment with NP KU60019 did significantly increase plasma AST concentrations compared to saline ($P < 0.05$), but there was no significant effect of particle size on the hepatotoxicity of either drug. A CBC of the mice demonstrated that Wtmn particles do cause significant decreases in white blood cells, but this effect was relatively small with no effect due to particle size. KU60019 nanoparticles had no effect on any CBC variables.

Liver Function

	Wortmannin		**KU60019**	
	AST	ALT	AST	ALT
Normal Range	30 – 60 U/L	30 – 60 U/L	30 – 60 U/L	30 – 60 U/L
Saline	57.5 +/- 6.2	36.8 +/- 3.1	57.5 +/- 6.2	36.8 +/- 3.1
50 nm	76.3 +/- 5.6	41.3 +/- 4.0	77.6 +/- 5.1*	33.6 +/- 2.2
100 nm	71.3 +/- 4.0	40.1 +/- 2.0	80.0 +/- 5.9*	39.6 +/- 1.3
150 nm	69.7 +/- 5.6	44.4 +/- 2.7	81.7 +/- 6.2*	37.2 +/- 1.3

Hematologic Profile

	Hb (g/dL)	**Hct (%)**	**RBC (10^6/µL)**	**Hb (g/dL)**	**Hct (%)**	**RBC (10^6/µL)**
Normal	10.1 – 16. 1	32.8 – 48	6.5 – 10.1	10.1 – 16.1	32.8 - 48	6.5 – 10.1
Saline	15.6 +/- 0.2	46.6 +/- 0.7	9.7 +/- 0.1	15.6 +/- 0.2	46.6 +/- 0.7	9.7 +/- 0.1
50 nm	15.8 +/- 0.4	45.9 +/- 0.8	9.8 +/- 0.2	15.4 +/- 0.2	45.2 +/- 1.0	9.6 +/- 0.2
100 nm	16.0 +/- 0.3	46.9 +/- 0.7	9.9 +/- 0.2	15.7 +/- 0.3	46.8 +/- 1.1	9.8 +/- 0.2
150 nm	15.8 +/- 0.4	46.1 +/- 0.5	9.6 +/- 0.2	15.2 +/- 0.2	45.3 +/- 0.8	9.5 +/- 0.2

	WBC (10^3/µL)	**Lymphocytes (10^3/µL)**	**Granulocytes (10^3/µL)**	**Monocytes (10^3/µL)**	**WBC (10^3/µL)**	**Lymphocytes (10^3/µL)**	**Granulocytes (10^3/µL)**	**Monocytes (10^3/µL)**
Normal	2.6 – 10.1	1.3 – 8.4	0.4 – 2.0	0 – 0.3	2.6 – 10.1	1.3 – 8.4	0.4 – 2.0	0 – 0.3

Saline	5.5 +/- 0.6	4.5 +/- 0.4	0.6 +/- 0.2	0.5 +/- 0.1	5.5 +/- 0.6	4.5 +/- 0.4	0.6 +/- 0.2	0.5 +/- 0.1
50 nm	2.8 +/- 0.8*	2.2 +/- 0.9*	0.2 +/- 0.1	0.3 +/- 0.1*	4.3 +/- 0.4	3.7 +/- 0.3	0.4 +/- 0.1	0.3 +/- 0.6
100 nm	2.9 +/- 0.6*	2.6 +/- 0.6*	0.1 +/- 0.1	0.2 +/- 0.1*	3.8 +/- 0.5	3.3 +/- 0.4	0.2 +/- 0.1	0.3 +/- 0.1
150 nm	3.0 +/- 0.8*	2.5 +/- 0.7*	0.2 +/- 0.1	0.3 +/- 0.1*	4.1 +/- 0.5	3.6 +/- 0.5	0.2 +/- 0.1	0.3 +/- 0.1

Table 2. Plasma levels of liver enzymes AST and ALT shown on top table (Wtmn left, KU60019 right). Peripheral blood values for specific hematologic values (hemoglobin (Hb), hematocrit (HCT), red blood cells (RBC), white blood cells (WBC), lymphocytes, granulocytes, and monocytes. *Significantly different from saline-treated controls.

Biodistribution

Effect of particle size on biodistribution was tested by injecting NPs labeled with a flamma fluor fluorescent tag and imaging organs (heart, liver, spleen, tumor xenograft) harvested at 1, 3, 6, 12, and 24 h after drug administration. Figure 6 depicts representative images of organs normalized to the unlabeled control background. The 150 nm particles rapidly accumulated in the liver and the spleen. The 100 nm particles accumulated more in the liver and spleen than the 50 nm particles, but less than the 150 nm particles. NPs of all sizes accumulated within tumors at similar overall average intensity levels but was most homogenous among the 50 nm particles.

Discussion

Several studies have shown the potential of nanoformulations of radiosensitizing drugs to improve the therapeutic index of CRT. However, very little is known about the optimal particle characteristics for use in CRT. Here, we compared the efficacy and toxicity of nanoparticles ranging from 50 – 150 nm in diameter, a size range consistent with nanoparticles currently in clinical development.[10] While our data does support previous publications that suggest sub-50 nm nanoparticles penetrate tumors more homogenously than larger particles, we were unable to demonstrate any therapeutic advantage to using sub-50 nm nanoparticles when combined with radiation. Our results suggest that using sub-50 nm NPs may not be optimal for use in CRT.

In addition to size, physical characteristics of particles which affect drug release kinetics are also important determinants of therapeutic efficacy in CRT. Particles of different sizes but

identical release rates were engineered to minimize the effects of variables other than size on

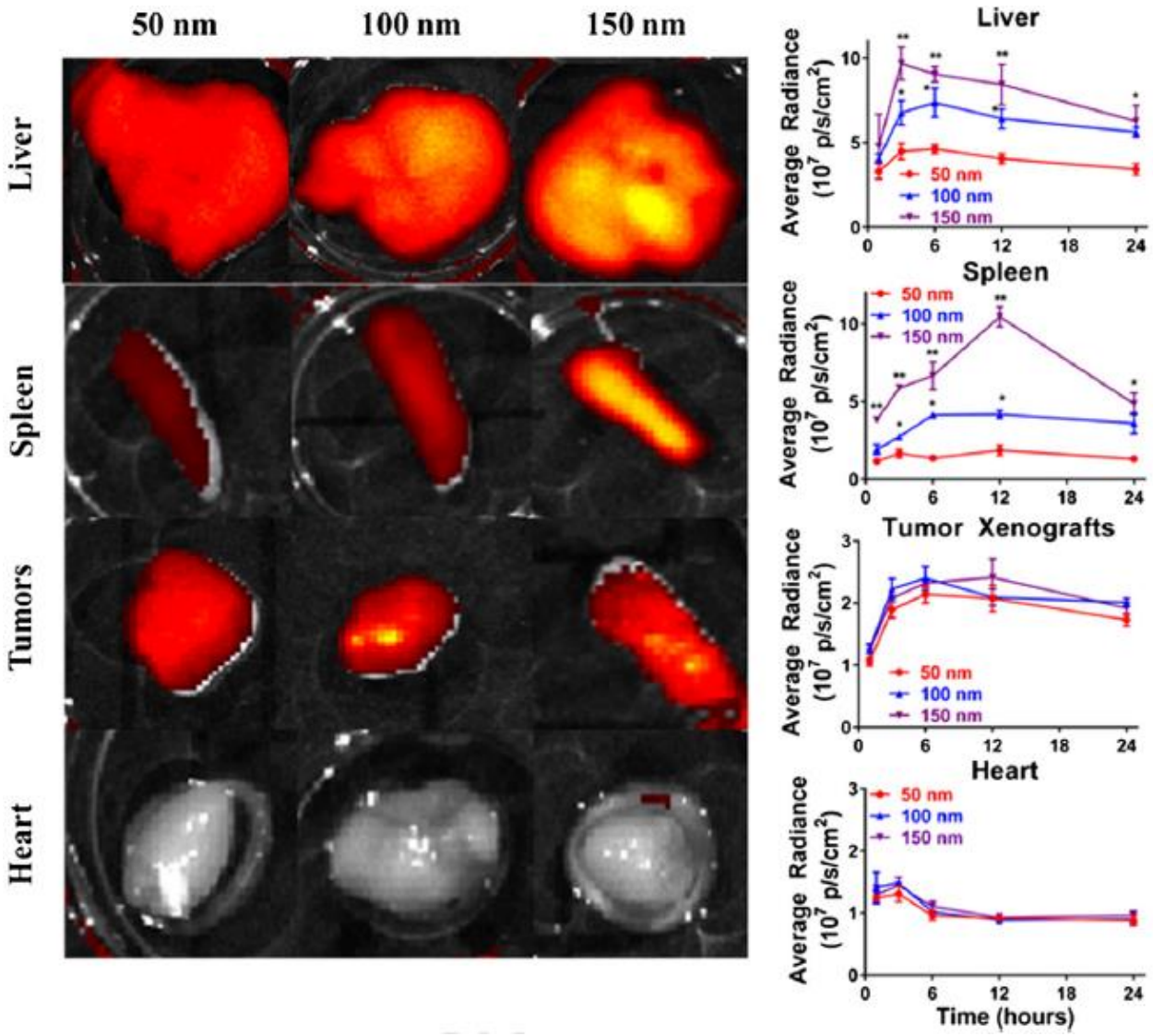

Figure 6. Effect of particle size on *in vivo* biodistribution. Background-normalized images of various organs harvested 6 h after *in vivo* administration of fluorescent-labeled nanoparticles (50 nm left, 100 nm middle, 150 nm right). Far right column shows accumulation of particles in the different organs at different times over 24 h. *Significantly more than 50 nm. **Significantly more than all other groups.

toxicity and efficacy. A particularly difficult variable to control for is drug sequestration within particles of different sizes. Small changes in particle diameter result in relatively large changes in particle volume ($V = 4/3\pi r^3$). Consequently, equal weights of polymer produce substantially fewer particles with considerably more drug per particle when formulating larger particles. How drug

sequestration within particles affects therapeutic efficacy and toxicity in CRT is unknown. It is possible that larger particles could at least partially offset poorer tumor penetration by delivering more drug per particle.

As chemotherapeutics, NP formulations of Wtmn and KU60019 had similar cytotoxic efficacies *in vitro* and that there was no effect due to particle size. When combined with radiation, NP formulations of KU60019 were substantially more toxic than Wtmn particles *in vitro*. Interestingly, this difference in efficacy between Wtmn and KU60019 particles with radiation was not observed *in vivo*. There are multiple significant differences between the two drug formulations which could affect their relative efficacy. For example, the two drugs have very different release kinetics, and the optimal time interval between radiation and particle administration *in vivo* is likely quite different between slow and fast releasing drugs. The purpose of this study was not to compare the relative efficacy of Wtmn and KU60019 nanoformulations, but rather to demonstrate that the effect of particle size on CRT was conserved across nanoformulations of different radiosensitizing drgus. the optimal administration of individual drugs will need to be considered on a case-by-case basis and is beyond the scope of this research.

We hypothesized that the smallest particles may have better therapeutic efficacy *in vivo*, since they should be more penetrating. However, in no instance was the 50 nm nanoformulation any more efficacious than the larger particles. Indeed, there was greater radiosensitization in the 100 nm nanoparticles. Differences in tumor penetration with particle size may partially explain this observation. Indirectly ionizing radiation (such as photons) is dependent upon sufficient oxygen levels in the immediate vicinity of the site of damage.[11] Tumor oxygenation is highly heterogeneous with areas of relatively high and low oxygenation and DNA repair inhibitors are only minimally sensitizing in the absence of oxygen.[12] By distributing homogeneously within

tumors, the smallest particles are indiscriminately localizing drug in oxygen-rich and hypoxic regions. In contrast, larger particles accumulate within the perivascular space, thus concentrating drug within the oxygenated tumor regions which are most likely to benefit from radiosensitization.[13] The 100 nm nanoparticles may be optimal because they provide the best balance between tumor penetration and perivascular accumulation. Whether this benefit is maintained over more protracted treatment schedules like those utilized in the clinic remains to be seen.

NP formulations of all sizes were well tolerated with CRT. Although it may be predicted that little leaking of 50 nm NPs through unaffected normal tissue vasculature would occur, it is possible that vascular damage caused by radiation may preferentially allow more tissue penetration of the 50 nm particles than the larger particles.[14] Toxicity in the GI tract specifically was studied because this area receives the highest doses of radiation during treatment for colorectal cancer.[15] No significant increase in radiation-induced toxicity was identified with the smallest particles. In fact, no particles of any size increased rectal toxicity compared to radiation alone. Some measurable systemic toxicity was observed in terms of increased plasma liver enzymes and decreased blood counts following nanoparticle administration. However, there was no effect due to particle size. Further, these effects were relatively small, and no mice demonstrated any obvious outward signs of treatment-related toxicity such as lethargy or weight loss.

In line with previous studies, we demonstrated that larger nanoparticles more rapidly accumulate in the liver and spleen.[16] By also measuring therapeutic efficacy and toxicity, two important observations were presented. First, increased hepatic and splenic clearance of larger particles does not translate into decreased efficacy with CRT. Even though a larger fraction of the total particle population is cleared, tumor accumulation still appears to be adequate with larger

particles. Second, increasing hepatic accumulations of particles encapsulating hepatotoxic drugs does not increase the hepatotoxicity of larger particles. Exactly how the liver clears drug from particles without incurring excess toxicity is currently unclear. The results of our study suggest that differences in biodistribution patterns with particle size do not necessarily translate into predictable changes in toxicity or efficacy when combined with radiation.

A few other limitations to this study should be considered. First, we engineered particles over a fairly large size range. It is possible that particle sizes between the tested ranges offer therapeutic advantages compared to the sizes actually tested in these experiments. Second, while we used a fractionated treatment regimen to mimic clinical delivery of CRT, this only consisted of 3 fractions of radiation and 2 injections of drug. Clinical CRT treatments tend occur over a longer and more separated period of time (20 – 30 fractions over 4 – 6 weeks),[17] and it is possible that changes in tumor or normal tissue vasculature in this setting may produce toxicity and/or efficacy profiles which more clearly favor a particular NP size. Finally, xenograft models of tumors were used, which have different physiological properties than native tumors, particularly with respect to the microenvironment surrounding the tumor. This likely limits our ability to extrapolate our results to spontaneously-occurring human tumors.

Conclusions

This study has demonstrated that nanoparticles encapsulating radiosensitizing drugs in clinically relevant size ranges (50 – 150 nm) are potent radiosensitizers and well-tolerated *in vivo*. Our results are the first to suggest that engineering sub-50 nm particles may not be optimal for use in chemoradiotherapy. While particle size has very clear effects on biodistribution and tumor penetration, its effects on antitumor efficacy when combined with radiation are more subtle and do not demonstrate any advantage to using small sized NPs. Indeed, when significant differences

in efficacy were observed, they favored the 100 nm nanoparticles over the other sizes. Whether this difference is observed in clinical practice or other model systems remains to be seen.

References

1. Karve, S., Werner, M. E., Sukumar, R., Cummings, N. D., Copp, J. A., Wang, E. C., ... & Wang, A. Z. (2012). Revival of the abandoned therapeutic wortmannin by nanoparticle drug delivery. *Proceedings of the National Academy of Sciences*, *109*(21), 8230-8235.
2. Brannon-Peppas, L., & Blanchette, J. O. (2012). Nanoparticle and targeted systems for cancer therapy. *Advanced drug delivery reviews*, *64*, 206-212.
3. Roedl, J. B., Colen, R. R., Holalkere, N. S., Fischman, A. J., Choi, N. C., & Blake, M. A. (2008). Adenocarcinomas of the esophagus: response to chemoradiotherapy is associated with decrease of metabolic tumor volume as measured on PET–CT: comparison to histopathologic and clinical response evaluation. *Radiotherapy and oncology*, *89*(3), 278-286.
4. Seiwert, T. Y., Salama, J. K., & Vokes, E. E. (2007). The concurrent chemoradiation paradigm—general principles. *Nature clinical practice Oncology*, *4*(2), 86-100.
5. Park, K. R., Monsky, W. L., Lee, C. G., Song, C. H., Kim, D. H., Jain, R. K., & Fukumura, D. (2016). Mast cells contribute to radiation-induced vascular hyperpermeability. *Radiation research*, *185*(2), 182-189.
6. Boulton, S., Kyle, S., Yalçintepe, L., & Durkacz, B. W. (1996). Wortmannin is a potent inhibitor of DNA double strand break but not single strand break repair in Chinese hamster ovary cells. *Carcinogenesis*, *17*(11), 2285-2290.
7. Lee, J. H., & Paull, T. T. (2005). ATM activation by DNA double-strand breaks through the Mre11-Rad50-Nbs1 complex. *Science*, *308*(5721), 551-554.
8. Winkler, F., Kozin, S. V., Tong, R. T., Chae, S. S., Booth, M. F., Garkavtsev, I., ... & Munn, L. L. (2004). Kinetics of vascular normalization by VEGFR2 blockade governs brain tumor response to radiation: role of oxygenation, angiopoietin-1, and matrix metalloproteinases. *Cancer cell*, *6*(6), 553-563.
9. Cascella, M., Cuomo, A., & Viscardi, D. (2016). Features and Management of the Pelvic Cancer Pain.
10. Min, Y., Caster, J. M., Eblan, M. J., & Wang, A. Z. (2015). Clinical translation of nanomedicine. *Chemical reviews*, *115*(19), 11147-11190.
11. Azzam, E. I., Jay-Gerin, J. P., & Pain, D. (2012). Ionizing radiation-induced metabolic oxidative stress and prolonged cell injury. *Cancer letters*, *327*(1), 48-60.
12. Wilson, W. R., & Hay, M. P. (2011). Targeting hypoxia in cancer therapy. *Nature Reviews Cancer*, *11*(6), 393-410.
13. Caster, J. M., Stephanie, K. Y., Patel, A. N., Newman, N. J., Lee, Z. J., Warner, S. B., ... & Wang, A. Z. (2017). Effect of particle size on the biodistribution, toxicity, and efficacy of drug-loaded polymeric nanoparticles in chemoradiotherapy. *Nanomedicine: Nanotechnology, Biology and Medicine*.
14. Begg, A. C., Stewart, F. A., & Vens, C. (2011). Strategies to improve radiotherapy with targeted drugs. *Nature Reviews Cancer*, *11*(4), 239-253.
15. Zelefsky, M. J., Levin, E. J., Hunt, M., Yamada, Y., Shippy, A. M., Jackson, A., & Amols, H. I. (2008). Incidence of late rectal and urinary toxicities after three-dimensional conformal radiotherapy and intensity-modulated radiotherapy for localized prostate cancer. *International Journal of Radiation Oncology* Biology* Physics*, *70*(4), 1124-1129.

16. Owens, D. E., & Peppas, N. A. (2006). Opsonization, biodistribution, and pharmacokinetics of polymeric nanoparticles. *International journal of pharmaceutics*, *307*(1), 93-102.
17. Bleehen, N. M., & Stenning, S. P. (1991). A Medical Research Council trial of two radiotherapy doses in the treatment of grades 3 and 4 astrocytoma. The Medical Research Council Brain Tumour Working Party. *British journal of cancer*, *64*(4), 769.

Abbreviations

ACN	Acetonitrile
CRT	Chemoradiotherapy
DMEM	Dulbecco's Modified Eagle Medium
DPBS	Dulbecco's phosphate-buffered saline
Gy	Gray (SI unit)
HPLC	High-pressure liquid chromatography
mPEG-PLGA	Methoxy-poly(ethylene glycol)-block-poly(lactic-co-glycolic acid)
NP	Nanoparticle
PBS	Phosphate-buffered saline
PDI	Polydispersity index
PLA	Poly(D,L-lactic acid)
TEM	Transmission electron microscopy
Wtmn	Wortmannin